Langmuir

Article

pubs.acs.org/Langmuir

Tridentate Adsorbates with Cyclohexyl Headgroups Assembled on Gold

Burapol Singhana, Supachai Rittikulsittichai, and T. Randall Lee*

Department of Chemistry and the Texas Center for Superconductivity, University of Houston, Houston, Texas 77204-5003, United States

ABSTRACT: The tridentate adsorbates cyclohexane-*cis*,*cis*-1,3,5-triyltrimethanethiol (**CyTSH**) and (*cis*,*cis*-1,3,5-trimethylcyclohexane-1,3,5-triyl)trimethanethiol (**3C1CyTSH**) were designed and synthesized. Thin films prepared by the adsorption of these molecules onto the surface of gold were characterized by ellipsometry, contact angle goniometry, polarization modulation infrared reflection absorption spectroscopy, and X-ray photoelectron spectroscopy (XPS). **CyTSH** was found to generate multilayer thin films with many unbound thiol species and oxidized sulfur moieties (e.g., disulfides and sulfones). In contrast, **3C1CyTSH** was found to generate monolayer films in which ∼90% of the thiols were bound to the surface of gold (∼10% unbound), and there were no oxidized sulfur species. In comparing **CyTSH** and **3C1CyTSH**, the methyl groups of **3C1CyTSH** impart rigidity to the structure, which significantly enhances the chemisorption of sulfur to the surface of gold. Ellipsometric measurements and analysis by XPS indicate that the thickness of the self-assembled monolayer formed from **3C1CyTSH** is ∼5 Å.

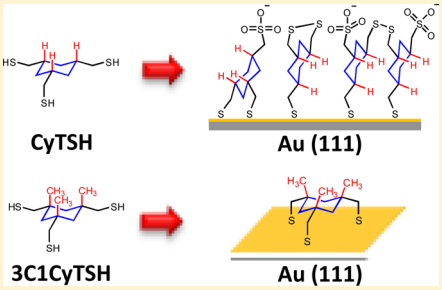

INTRODUCTION

Self-assembled monolayers (SAMs) are formed when amphiphilic molecules adsorb spontaneously onto the surface of an appropriate substrate. In particular, SAMs generated by the adsorption of alkanethiols on gold have been widely studied because of their facile generation, manipulation, and characterization.[1−5] Furthermore, these SAMs have found use in a variety of applications, such as corrosion resistance,[6] biomaterial coatings,[7] biosensors,[8] and nanomedicine,[9−11] as well as adhesion,[12] friction and lubrication,[13,14] lithographic patterning,[15,16] electrode modification,[17] and thin-film transistor applications.[18−20]

Despite the attractive properties of SAMs, their somewhat fragile nature remains a critical drawback for many applications.[21−24] While some studies have reported that alkanethiolate SAMs exhibit moderate stability at room temperature, others have noted that SAMs desorb upon exposure to air in the absence of light over a span of a few days.[25] Moreover, normal alkanethiol-based SAMs decompose rapidly upon heating at elevated temperatures (e.g., 80 °C in hexadecane).[5,21,24,26] They also readily undergo displacement when exposed to organosulfur adsorbates in solution.[21,24]

To circumvent this problem, researchers have explored several strategies for generating thermally and chemically stable SAMs. One such strategy employed by our research team[5,21,24,26−32] and others[33−36] utilizes adsorbates with the capacity for multiple sulfur−gold interactions, which can afford SAMs with enhanced stability through the entropically driven "chelate effect".[21,24,26,28,30] Further, chelating adsorbates can be designed to resist the formation of intramolecular disulfides upon desorption from the surface, which provides additional stability to such multidentate SAMs.[21,24,26,28,30]

During the course of our earlier studies, we examined the stability of multidentate organosulfur adsorbates both on evaporated "flat" gold and on gold nanoparticles. As a whole, we found that SAMs generated from tridentate adsorbates are more thermally stable than those generated from bidentate adsorbates, which in turn are more stable than those generated from monodentate adsorbates.[30,37] Furthermore, independent studies have found that long-chain alkanethiols fail to displace tridentate adsorbates under conditions where monodentate adsorbates were readily displaced.[24,38] Of particular relevance, two adamantane-based tridentate adsorbates were used to generate SAMs on gold (see Figure 1a,b);[38−40] for these adsorbates, all three thiomethyl legs bind to gold in a fashion similar to normal alkanethiols.[39,40] However, save for their noted resistance to displacement,[38] there have been no reports of the stability of the films generated from these adsorbates.

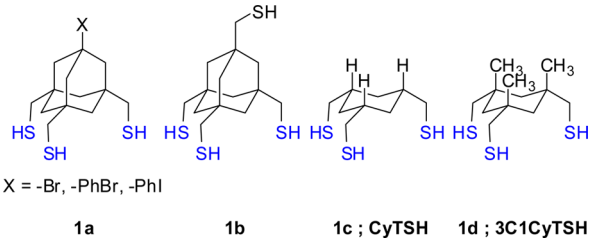

Figure 1. Structures of tridentate adsorbates with cyclohexyl headgroups.

Received: July 31, 2012
Revised: October 8, 2012
Published: December 3, 2012

Scheme 1. Synthesis of Tridentate Adsorbates 3C1CyTSH and CyTSH

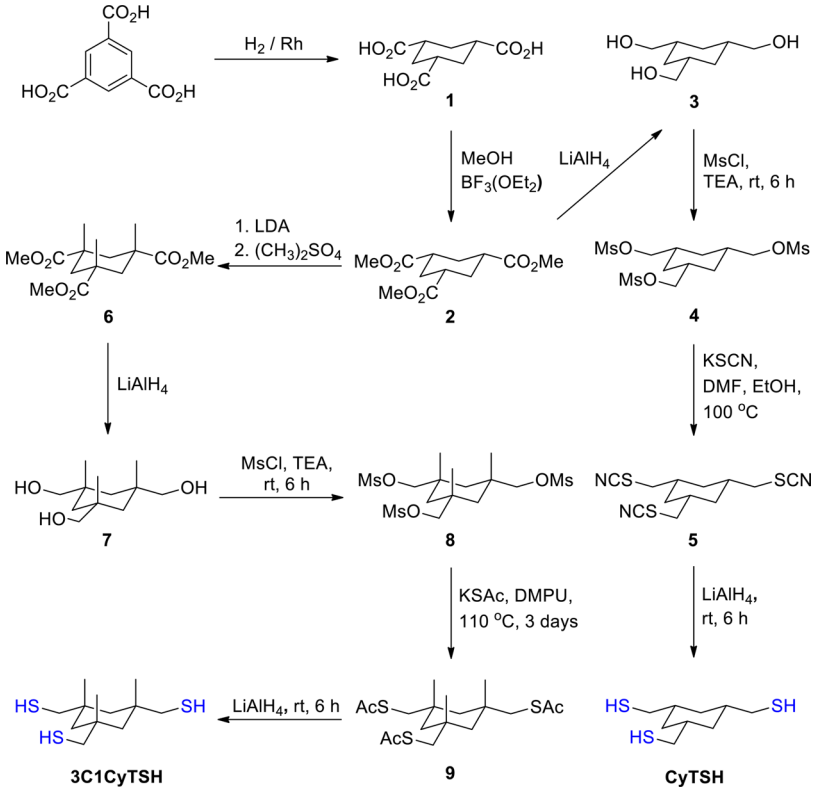

In an effort to generate a synthetically accessible and chemically versatile class of multidentate thiol for preparing stable, well-defined SAMs on gold, we chose in the present study to explore a new adsorbate architecture in which a cyclohexane ring serves as a framework for linking thiol headgroups with synthetically variable tailgroups. Figure 1c,d shows the chemical structure of the first two examples of this class of adsorbate, where the top of the cyclohexane ring is unmodified (1c; **CyTSH**) or modified with three symmetrically equivalent methyl groups (1d; **3C1CyTSH**).

There are at least five reasons that motivated us to choose a cyclohexane ring as the linking moiety. First, we anticipated that the geometry afforded by the 1,3,5-substituted cyclohexane ring would allow for adsorption of the headgroups to the surface of gold and simultaneous direction of the tailgroups away from the surface. Second, the three thiomethyl legs of the chelating adsorbate can plausibly bind simultaneously to the gold surface, thereby affording films with enhanced stability. Third, two or three distinct functional groups could be incorporated into the tailgroups of this adsorbate to afford chemically unique hybrid surfaces with functional groups that are homogeneously mixed at the molecular level (rather than phase separated). Fourth, we anticipated that the steric bulk of the cyclohexyl moiety would be sufficiently small to allow dense packing of the tailgroups and concomitant van der Waals stabilization. Finally, in contrast to the tridentate adamantanethiols, which fail to form well-packed films due to insufficient interchain van der Waals interactions,[39] our tridentate cyclohexyl-based alkanethiols can be synthesized to possess long alkyl tailgroups.

As part of our initial efforts to evaluate the capacity of these tridentate cyclohexyl-based alkanethiols to form SAMs, we describe in this report the self-assembly of **CyTSH** and **3C1CyTSH** on the surface of gold. We characterize the resultant films by ellipsometry, contact angle goniometry, polarization modulation infrared reflection absorption spectroscopy (PM-IRRAS), and X-ray photoelectron spectroscopy (XPS).

EXPERIMENTAL SECTION

Materials. Gold (99.9%) shot was purchased from Americana Precious Metals. Chromium rods (99.9%) were obtained from R. D. Mathis Company. Polished single-crystal Si(100) wafers were purchased from NESTEC and rinsed with absolute ethanol (Aaper Alcohol and Chemical Co.) before use. 1,3,5-Benzenetricarboxylic acid (95%), 5% rhodium on activated alumina, boron trifluoride diethyl etherate, methanesulfonyl chloride (puriss, ≥ 99.0%), potassium thioacetate (98%), potassium thiocyanate (ACS reagent, ≥ 99.0%), dimethyl sulfate (≥99.8%), and 1,3-dimethyl-3,4,5,6-tetrahydro-2(1H)-pyrimidinone (absolute, over molecular sieve, ≥ 99.0%) were purchased from Sigma–Aldrich. Lithium aluminum hydride ($LiAlH_4$) was obtained from Alfa Aesar. All reagents were used as received without further purification unless otherwise specified.

Synthesis of Tridentate Alkanethiol Adsorbates. The adsorbates cyclohexane-*cis*,*cis*-1,3,5-triyltrimethanethiol (**CyTSH**) and (*cis*,*cis*-1,3,5-trimethylcyclohexane-1,3,5-triyl)trimethanethiol (**3C1CyTSH**) were prepared using the strategy outlined in Scheme 1. Detailed experimental procedures and spectroscopic data are provided in the following paragraphs. While we provide only ^{1}H NMR spectral data are for each of the intermediates, we provide a more complete characterization (^{1}H NMR spectroscopy, ^{13}C NMR spectroscopy, FT-IR spectroscopy, and mass spectrometry) for the final adsorbate products **CyTSH** and **3C1CyTSH**.

***cis*,*cis*-Cyclohexane-1,3,5-tricarboxylic Acid (1).**[41] A mixture of 7.50 g (3.57 mmol) of trimesic acid, 1.0 g of 5% rhodium on alumina, and 150 mL of water was hydrogenated at 70 °C and 50 psi of H_2. Uptake was complete in 48 h, and the filtrate was concentrated to give a white solid. Recrystallization from a 1:4 mixture of ethanol/toluene gave 4.50 g (20.8 mmol) of the *cis*,*cis* isomer (58% yield). ^{1}H NMR

dx.doi.org/10.1021/la303101x | *Langmuir* 2013, 29, 561–569

(500 MHz, CD_3OD): δ 12.22 (br, 3H; 3COO*H*), 2.32 (tt, J = 3, 13 Hz; 3H, 3H_{ax}′), 2.04 (d, J = 13 Hz, 3H; 3H_{eq}), 1.19 (q, J = 13 Hz, 3H; 3H_{ax}).

***cis,cis*-Trimethylcyclohexane-1,3,5-tricarboxylate (2).** Anhydrous methanol was distilled over CaH_2 before use. *cis,cis*-Cyclohexane-1,3,5-tricarboxylic acid **1** (1.0 g, 4.6 mmol) was heated under reflux for 6 h with boron trifluoride diethyl etherate (4.2 g, 30 mmol) in an excess of dry methanol (50 mL). The reaction mixture was cooled and poured into a saturated sodium bicarbonate solution. The organic phase was then extracted with diethyl ether and dried over Na_2SO_4. Removal of the ether afforded the crude trimethyl ester (1.05 g, 4.07 mmol, 88% yield). ^{1}H NMR (400 MHz, CD_3OD): δ 3.68 (s, 9H; 3COOCH_3), 2.36 (tt, J = 3, 13 Hz; 3H, 3H_{ax}′), 2.25−2.29 (m, 3H; 3H_{eq}), 1.53 (q, J = 13 Hz, 3H; 3H_{ax}).

Cyclohexane-*cis,cis*-1,3,5-trimethanol (3).[42] A slurry of $LiAlH_4$ (2.0 g, 53 mmol) in 50 mL of dry THF was placed in a 250 mL three-necked round-bottomed flask equipped with an addition funnel and purged with nitrogen at room temperature (rt). A slight evolution of gas was observed. The addition funnel was charged with *cis,cis*-trimethylcyclohexane-1,3,5-tricarboxylate **2** (2.23 g, 8.63 mmol) in 70 mL of THF. The solution of **2** was added to the solution of LAH over 15 min at rt, which led to a vigorous evolution of gas. The solution was refluxed for 8 h and was then cooled to rt and quenched sequentially with water (2 mL), 15% aq NaOH (2 mL), and water (8 mL). A white precipitate formed, and the mixture was stirred for an additional 2 h at rt. The solution was filtered through Celite, and the pad was washed with THF (5 × 100 mL). The filtrate was dried over Na_2SO_4, filtered, and reduced in vacuo to give **3** as a white solid (1.20 g, 6.89 mmol, 80% yield). ^{1}H NMR (500 MHz, CD_3OD): δ 3.38 (d, J = 8 Hz, 6H; 3CH_2OH), 1.85 (d, J = 14 Hz, 3H; 3H_{eq}), 1.51 (m, 3H; 3H_{ax}′), 0.54 (q, J = 14 Hz, 3H; 3H_{ax}).

Cyclohexane-*cis,cis*-1,3,5-triyltris(methylene)-trimethanesulfonate (4). The trialcohol **3** (0.60 g, 3.4 mmol) in dry THF (100 mL) was treated with triethylamine (20 mL, 143 mmol) and stirred for 10 min at rt. Methanesulfonyl chloride (1.10 mL, 11.6 mmol) was then added dropwise over a period of 15 min. The reaction mixture was stirred for 6 h under nitrogen and then transferred to a separatory funnel. After adding water into the mixture to decompose any remaining methanesulfonyl chloride, the mixture was extracted with dichloromethane (DCM, 3 × 100 mL). The combined organic phases were successively washed with 2 N HCl and H_2O and then dried over $MgSO_4$. The DCM solution was concentrated to give the crude product, which was recrystallized from 3:1 hexane/DCM to obtain **4** as a yellowish solid (1.25 g, 3.06 mmol, 89% yield). ^{1}H NMR (400 MHz, CD_3Cl): δ 4.08 (d, J = 6 Hz, 6H; 3$CH_2OSO_2CH_3$), 3.02 (s, 9H; 3OSO$_2CH_3$), 1.48 (m, 6H; 3H_{ax}′ + 3H_{eq}), 0.88 (d, J = 12 Hz, 3H; 3H_{ax}).

***cis,cis*-1,3,5-Tris(thiocyanatomethyl)cyclohexane (5).** A mixture of **4** (0.520 g, 1.30 mmol) and potassium thiocyanate (KSCN, 4.9 g, 50 mmol) was dissolved in ethanol and DMF (1:1) and then refluxed overnight at 100 °C. The solution was then cooled to rt, water was added, and the mixture was extracted with DCM (3 × 30 mL). The combined organic phases were washed several times with water to remove the DMF. After washing with brine, the organic layer was dried over $MgSO_4$. The solvent was evaporated, and a pale yellow solid was obtained, which was recrystallized twice from a 1:3 mixture of DCM and MeOH to give pure **5** (0.26 g, 0.87 mmol, 68% yield). ^{1}H NMR (500 MHz, CD_3Cl): δ 2.94 (d, J = 6 Hz, 6H; 3CH_2SCN), 2.17 (d, J = 12 Hz, 3H; 3H_{eq}), 1.95 (m, 3H; 3H_{ax}′), 0.86 (q, J = 12 Hz, 3H; 3H_{ax}).

Cyclohexane-*cis,cis*-1,3,5-triyltrimethanethiol (CyTSH). To a suspension of $LiAlH_4$ (0.33 g, 8.70 mmol) in dry THF (10 mL) was added dropwise a solution of **5** (0.26 g, 0.87 mmol) in dry THF. The reaction was stirred at rt for 6 h and then quenched with H_2O and acidified with 2 M HCl under nitrogen (H_2O and 2 N HCl were degassed by bubbling with nitrogen before use). After stirring for 10 min, the reaction mixture was extracted with DCM (3 × 20 mL). The combined organic layers were washed with H_2O and brine. After drying the solution with Na_2SO4, the solvent was removed by rotary evaporation to afford **CyTSH** as a clear oil (0.16 g, 0.72 mmol, 82% yield). ^{1}H NMR (500 MHz, CD_3Cl): δ 2.47 (m, 6H; 3CH_2SH), 2.01 (d, J = 12 Hz, 3H; 3H_{eq}), 1.52 (m, 3H; 3$H_{ax'}$), 1.32 (t, J = 8 Hz, 3H; 3S*H*), 0.65 (q, J = 12 Hz, 3H; 3H_{ax}). ^{13}C NMR (125 MHz, CD_3Cl): δ 40.27, 37.00, 31.33. IR (neat oil): 2915, 2892, 2841, 2560 cm^{-1}.

Trimethyl-*cis,cis*-1,3,5-trimethylcyclohexane-1,3,5-tricarboxylate (6)..[41,43] Diisopropylamine was dried over molecular sieves before use. Lithium diisopropylamide (LDA) was generated at 0 °C by the addition of 2.5 M BuLi in hexanes (5.11 mL, 12.8 mmol) to diisopropylamine (1.80 mL, 12.8 mmol) in 10 mL of dry diethyl ether. To the remaining mixture was added dropwise 1.0 g (3.9 mmol) of the *cis,cis*-trimethylcyclohexane-1,3,5-tricarboxylate **2** in 10 mL of diethyl ether. The mixture was stirred at 0 °C for 2 h. Then, 2 mL (21 mmol) of dimethylsulfate was added, and stirring was continued overnight at rt. The solution was washed with water, 1 N HCl, and brine, and it was dried over Na_2SO_4. After removal of the volatiles, 0.85 g of oil was obtained. Fractional recrystallization from 1:1 pentane/diethyl ether afforded the pure *cis,cis* isomer as a white solid (0.54 g, 1.8 mmol, 47% yield). ^{1}H NMR (300 MHz, $CDCl_3$): δ 3.66 (m, 9H; 3CO_2CH_3), 2.73 (d, J = 15 Hz, 3H; 3H_{eq}), 1.21 (m, 9H; 3CH_3), 0.96 (d, J = 15 Hz, 3H; 3H_{ax}).

(*cis,cis*-1,3,5-Trimethylcyclohexane-1,3,5-triyl)trimethanol (7). This intermediate was prepared in 88% yield as a white solid (0.63 g, 2.9 mmol) from **6** (1.0 g, 3.3 mmol) and $LiAlH_4$ (1.8 g, 48 mmol) in dry THF (20 mL) using the procedure described above for the synthesis of **3**. ^{1}H NMR (300 MHz, CD_3OD): δ 3.12 (s, 6H; 3CH_2OH), 1.22 (d, J = 14 Hz, 3H; 3H_{eq}), 1.08 (m, 12H; 3CH_3 + 3H_{ax}).

(*cis,cis*-1,3,5-Trimethylcyclohexane-1,3,5-triyl)tris-(methylene)trimethanesulfonate (8). This intermediate was prepared in 90% yield as a white solid (2.27 g, 5.04 mmol) from trialcohol **7** (1.21 g, 5.59 mmol) in dry THF (100 mL), triethylamine, and methanesulfonyl chloride (3.9 g, 31 mmol) using the procedure described above for the synthesis of **4**. ^{1}H NMR (300 MHz, $CDCl_3$): δ 3.91 (s, 6H; 3$CH_2OSO_2CH_3$), 3.12 (s, 9H; 3OSO$_2CH_3$), 1.48 (d, J = 14 Hz, 3H; 3H_{eq}), 1.34 (d, J = 14 Hz, 3H; 3H_{ax}), 1.32 (s, 9H; 3CH_3).

(*cis,cis*-1,3,5-Trimethylcyclohexane-1,3,5-triyl)tris-(methylene)triethanethiolate (9). A mixture of **8** (0.859 g, 1.90 mmol) and potassium thioacetate (KSAc, 6.53 g, 57.2 mmol) in anhydrous DMPU (30 mL) was stirred at 110 °C for 3 days. After cooling to rt, the solution was poured into water and extracted with DCM (3 × 100 mL). The combined organic phases were washed with water several times to remove the DMPU and then washed with saturated brine, dried over $MgSO_4$, and concentrated to dryness. The crude product was purified by column chromatography on silica gel, eluting with a mixture of 8.3% ethyl acetate in hexanes to afford **9** as a colorless liquid (0.21 g, 0.54 mmol, 28% yield). ^{1}H NMR (300 MHz, $CDCl_3$): δ 2.79 (s, 6H; 3CH_2SCOCH$_3$), 2.36 (s, 9H; 3SCOCH_3), 1.33 (d, J = 14 Hz, 3H; 3H_{eq}), 1.11 (m, 12H; 3CH_3 +3H_{ax}).

(*cis,cis*-1,3,5-Trimethylcyclohexane-1,3,5-triyl)-trimethanethiol (3C1CyTSH). The final product was obtained as an oil in 74% yield (0.105 g, 3.97 mmol) by treating compound **9** (0.21, 0.54 mmol) with $LiAlH_4$ (0.061 g, 1.6 mmol) in dry THF (10 mL) as described above in the synthesis of **CyTSH**. ^{1}H NMR (500 MHz, CD_3Cl): δ 2.39 (d, J = 9 Hz, 6H; 3CH_2SH), 1.35 (d, J = 14 Hz, 3H; 3H_{eq}), 1.25 (t, J = 9 Hz, 3H; 3S*H*), 1.18 (m, 12H; 3CH_3 + 3H_{ax}). ^{13}C NMR (125 MHz, CD_3Cl): δ 44.95, 42.11, 35.03, 26.70. IR (KBr, neat): 3100, 2952, 2911, 2558 cm^{-1}.

Substrate Preparation. Gold surfaces were prepared by the thermal evaporation of chromium (ca. 100 Å) under high vacuum at a pressure of ~6 × 10^{-5} Torr onto silicon wafers. Chromium was used as a primer to promote the adhesion of gold to the surface of silicon. A gold film having a thickness of approximately 2000 Å was deposited on the chromium at a rate of 1 Å/s. The substrates were rinsed with absolute ethanol and dried under a stream of ultrapure nitrogen before use.[29,30,44]

Preparation of SAMs. Solutions of the thiols were prepared in weighing bottles that were cleaned by soaking overnight in "piranha solution" (3:1 mixture of concentrated H_2SO_4/30% H_2O_2). *Caution: "piranha solution" reacts violently with organic materials and should be handled carefully.* The bottles were then thoroughly rinsed with deionized water and absolute ethanol and then dried overnight at 100

dx.doi.org/10.1021/la303101x | *Langmuir* 2013, 29, 561−569

°C. The gold-coated wafers were cut into slides (ca. 1 cm × 3 cm) and then rinsed with absolute ethanol and blown dry with ultrapure nitrogen before immersing in the thiol solutions. All substrates were allowed to equilibrate for a period of 48 h. The resultant SAMs were thoroughly rinsed with THF and absolute ethanol and then blown dry with ultrapure nitrogen before characterization.

Measurements of Ellipsometric Thickness. The thicknesses of the monolayers were measured using a Rudolf Research Auto ELIII ellipsometer equipped with a He−Ne laser operating at 632.8 nm and an incident angle of 70°. The optical constants of the bare gold were measured immediately after evaporation. For each sample, data collected from measurements on two separate slides with at least three spots per slide were averaged. The thicknesses of the monolayers were calculated assuming a refractive index of 1.45 for all monolayers. The thickness values obtained by ellipsometry were compared to those calculated from XPS measurements (vide infra).

Contact Angle Measurements. Contact angles were measured using a Rame′-Hart model 100 contact angle goniometer at room temperature (ca. 293 K). The contacting liquids (water, hexadecane, decalin, and diisopropyl ether) were dispensed and withdrawn using a Matrix Technologies micro-Electrapette 25 operated at the slowest possible speed (ca. 1 μL/s), and the advancing angle (θ_a) was measured while the pipet tip was kept in contact with the drop. For each type of monolayer film, contact angles were averaged from the collected measurements on two separate slides using at least three drops per slide.

Fourier Transform IR Spectroscopy. The bulk IR spectrum of **3C1CyTSH** was collected using a Nicolet Nexus-IR 670 Fourier transform (FT) spectrometer. A 500 mg portion of dry spectra-grade KBr was ground in a clean mortar and pressed to 10 000−15 000 pounds under vacuum. The sample was held at this pressure for 5 min. A few drops of **3C1CyTSH** were added onto the KBr pellet, and ultrapure nitrogen was blown across the surface. The KBr pellet containing the sample was mounted on a sample holder, and the spectrum was recorded using 32 scans.

Polarization Modulation IR Reflection Absorption Spectroscopy. The surface IR spectra were collected employing a Nicolet Nexus 670 Fourier transform spectrometer equipped with a liquid-nitrogen cooled mercury−cadmium−telluride (MCT) detector and a Hinds Instruments PEM-90 photoelastic modulator operating at 37 kHz. The polarized light was reflected from the sample at an angle of incidence of 80°. The spectra were collected over 256 scans at a spectral resolution of 4 cm^{-1}.

X-ray Photoelectron Spectroscopy Measurements. XPS spectra of the monolayer films were obtained using a PHI5700 X-ray photoelectron spectrometer equipped with a monochromatic Al Kα X-ray source ($h\nu$ = 1486.7 eV) incident at 90° relative to the axis of a hemispherical energy analyzer. The instrument was operated at high resolution with a pass energy of 23.5 eV and a photoelectron takeoff angle of 45° from the surface. All spectra were collected at room temperature. After collecting the spectra, the binding energy of $Au4f_{7/2}$ was set at 84.0 eV as a reference binding energy for standard calibration of all of the samples. The peak intensities were quantified by standard curve-fitting software using Shirley background subtraction and Gaussian−Lorentzian profiles. All of the peaks were fit with respect to spin−orbit splitting; specifically, two 80% Gaussian curves in a 1:2 ratio of areas split at 1.18 eV were used for analysis of the S_{2p} peaks. Based on these measurements, we estimate the accuracy of the reported percentages of bound versus unbound thiol to be no better than ±5%.

RESULTS AND DISCUSSION

Synthesis of New Tridentate Adsorbates. The adsorbates **3C1CyTSH** and **CyTSH** were prepared using the strategy outlined in Scheme 1. The compounds were identified by ^1H and ^{13}C NMR spectroscopies, FT-IR spectroscopy, and mass spectrometry, all of which confirmed their proposed structures.

Sulfur−Gold Chemisorption and Binding Energy Analysis by XPS. Based on previous electron diffraction and low energy helium diffraction studies of the structure of normal alkanethiolate SAMs on gold,[1−4] the sulfur−sulfur spacing is ∼5 Å with the sulfur atoms bound to the 3-fold hollow sites on Au(111).[1−4] To the best of our knowledge, there have been no reports of adsorbates having a cyclohexane framework such as those shown in Figure 1c,d. However, we note that the structurally related adamantanetrithiol derivatives reported by Whitesell and Kitagawa (Figure 1a,b)[38−40] form SAMs on gold with an S−S spacing of ∼5.0 Å, which is identical to the interatomic distance between sulfur atoms in normal alkanethiolate SAMs on Au(111).[1−4] Based on scanning tunneling microscopy data, the authors proposed that all three sulfur atoms of the adamantanetrithiols were bound to the surface of gold.[39,40]

These previous studies led us to hypothesize that **CyTSH** and **3C1CyTSH** would also generate SAMs on gold with all three sulfur atoms bound to gold—a condition essential for generating stable monolayer coatings. We therefore sought to characterize the nature of the sulfur atoms in films derived from **CyTSH** and **3C1CyTSH**. To this end, we explored the use of various solvents from which to generate optimal SAMs from these adsorbates, relying on studies by XPS to characterize the nature of sulfur−gold binding (i.e., bound vs unbound thiol). Further, because our ultimate studies will utilize SAMs formed from adsorbates with long and chemically varied tailgroups, we focused our initial survey studies on thin films formed from **CyTSH** and particularly **3C1CyTSH**.

The chemisorption between sulfur and gold surfaces in SAMs can be monitored using the XPS binding energies, which can be used to determine more broadly the chemical composition on the surface.[30,45] Thus, by monitoring the S_{2p} region of the XPS spectra, the binding of the sulfur headgroup to the gold substrate can be evaluated.[45−47] In the XPS spectra of SAMs generated from alkanethiols on gold, the binding energy of the $S_{2p^3/2}$ and $S_{2p^1/2}$ peaks for thiols bound to gold is known to be 162 and 163.2 eV, respectively.[47] In contrast, the $S_{2p^3/2}$ and $S_{2p^1/2}$ peaks for unbound thiols or disulfide species on the surface appear roughly at 164 and 165 eV, respectively.[45] Therefore, incomplete adsorbate binding on gold can be identified and quantified by the presence of the S_{2p} peak at 164 eV.[47] Moreover, oxidized sulfur species (S_{2p} BE > 166 eV) can also be detected by XPS.[30,47] Thus, we used XPS to characterize the SAMs generated from **3C1CyTSH** upon adsorption from various organic solvents (Figure 2).

Previous studies of the generation of SAMs from multidentate adsorbates have found that the solvent used for the adsorption can strongly influence the percentage of bound versus unbound sulfur in the resultant SAM.[21,24,26−30] To this end, we first explored the use of ethanol as a solvent from which to adsorb **3C1CyTSH** because ethanol is the most widely used solvent for preparing SAMs on gold. The popularity of ethanol can be attributed to its relatively low price, its availability in high purity, and its low toxicity. In addition, ethanol has a low tendency to be incorporated into SAMs[30,48] and is known to form robust and fully bound normal alkane mono-, di-, and trithiols SAMs on gold.[29] Other solvents that we used to adsorb **3C1CyTSH** onto gold included the polar aprotic solvents THF and DMF, which have been used previously to form fully bound bidentate and tridentate SAMs

dx.doi.org/10.1021/la303101x | Langmuir 2013, 29, 561−569

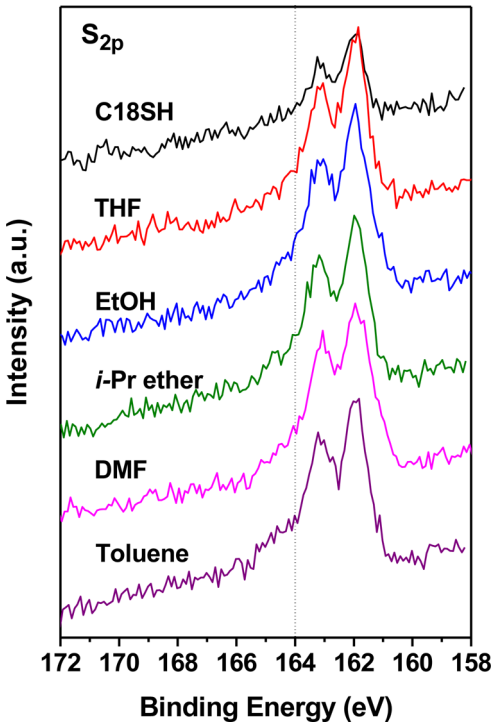

Figure 2. XPS spectra of the S_{2p} region for SAMs derived from **3C1CyTSH** in the indicated solvents.

on gold.[30] We also examined the adsorption of **3C1CyTSH** from isopropyl ether and toluene.

For all of these studies, the gold substrates were immersed in 1 mM solutions of **3C1CyTSH** and allowed to equilibrate for 48 h. The slides were exhaustively rinsed with THF, toluene, and ethanol and then dried under a vigorous stream of ultrapure nitrogen before analysis by XPS.

The XPS spectra of SAMs generated from **3C1CyTSH** in various solvents are shown in Figure 2, with a focus on the S_{2p} region. For all of the samples, the S_{2p} peaks exhibit some degree of intensity at 164 eV, indicating incomplete binding of the adsorbate to gold. The relative amounts of bound and unbound sulfur were deconvoluted using standard XPS software processing and are summarized in Table 1. Although none of

Table 1. Relative Amounts of Bound vs Unbound Sulfur Species Obtained from Deconvolution of the XPS Spectra in Figure 2

adsorbate	solvent	% bound thiolate	% unbound thiol
3C1CyTSH	THF	89	11
3C1CyTSH	EtOH	79	21
3C1CyTSH	*i*-Pr ether	73	27
3C1CyTSH	DMF	70	30
3C1CyTSH	toluene	68	32

the samples show completely bound thiolates for **3C1CyTSH**, the adsorption from THF appears to be optimal, with ~90% of the sulfur atoms bound to gold. Although a comprehensive understanding of the mechanism by which the solvent influences the formation of SAMs on gold remains obscure,[1] the good solubility of the adsorbates in THF, together with the ability of polar solvents such as THF to stabilize partial charge separation in the adsorption step,[49] might contribute to the observed superior performance of THF in the generation of SAMs on gold from **3C1CyTSH**.

To examine whether the methyl groups play any role in the chemisorption of sulfur to gold, we prepared the **CyTSH** film in the same manner as that used to prepare the optimal **3C1CyTSH** SAM (i.e., using THF as a solvent). XPS spectra of the S_{2p} region for the **CyTSH** films are displayed in Figure 3c, together with the corresponding data for SAMs derived analogously from octadecanethiol (Figure 3a) and **3C1CyTSH** (Figure 3b). The XPS spectra of the films derived from **CyTSH** (Figure 3c) show a high intensity S_{2p} peak at ~164 eV, indicating substantial unbound thiol and/or disulfide species (~80%) and some bound thiolate (~20%) in the film. Further, the peaks at 166−170 eV suggest the presence of oxidized sulfur species (e.g., sulfones).[45,47] Based on our observations, molecular **CyTSH** is stable under ambient conditions. However, SAMs derived from **CyTSH** readily undergo partial oxidition when exposed to oxygen and light.[50] In an effort to decrease the amount of oxidized sulfur species, we generated films from **CyTSH** in degassed THF, under nitrogen, and in the absence of light for 48 h at room temperature. Under these "inert" conditions, we found that the amount of oxidized sulfur species and unbound thiol (~60%) decreased, while the amount of bound thiolate (~40%) increased (see Figure 3d).

On the whole, comparison of the data collected for SAMs derived from **3C1CyTSH** and **CyTSH** suggests that the methyl groups on the cyclohexane ring of **3C1CyTSH** significantly enhance the chemisorption of sulfur to gold for this class of adsorbate. It is possible, for example, that the presence of the methyl groups gives rise to minor conformers in which the methylene thiol moieties occupy axial positions (Scheme 2).[51,52] This arrangement facilitates the binding of the thiols to gold. In contrast, the absence of the methyl groups in **CyTSH** gives rise to exclusively equatorial conformations for the methylene thiols, which allows for one or more of the methylene thiols to orient away from the surface upon initial chemisorption. This hypothesis is consistent with the XPS data shown in Figure 3. Finally, the presence of oxidized sulfur species (e.g., disulfides and sulfones) in the films formed from **CyTSH** is likely due to oxidation of the unbound thiols of **CyTSH** (vide supra). Finally, although the axial hydrogens of bound **3C1CyTSH** might come close to the surface of gold, this potential interaction appears to give rise to no significant repulsion, which is supported by the observed high percentage of bound thiolate indicated by XPS for this SAM when adsorbed from THF (~90%).

Chemical and Orientational Analysis by IR Spectroscopy. Figure 4 shows the spectra collected by transmission IR spectroscopy and PM-IRRAS for neat **3C1CyTSH** and for the SAM derived from this adsorbate. The S−H vibrations, observed at ~2558 cm^{-1} in the neat transmission IR spectrum,[39] were absent in the PM-IRRAS spectrum of the SAMs (Figure 4). The loss of the S−H peaks upon adsorption is consistent with the molecules attaching to gold via the three sulfur atoms in a tripodlike, perpendicular orientation.[39]

For many SAMs, the molecular orientation can be elucidated by monitoring the C−H stretching region of the surface IR spectra.[27,29,30,53,54] In most cases, the frequency, bandwidth, and intensity of the methylene antisymmetric and symmetric bands ($\nu_a^{CH_2}$ at ~2918 cm^{-1} and $\nu_s^{CH_2}$ at ~2850 cm^{-1}) and the methyl antisymmetric and symmetric bands ($\nu_a^{CH_3}$ at ~2956 cm^{-1} and $\nu_s^{CH_3}$ at ~2866 cm^{-1}) are strongly influenced by the

dx.doi.org/10.1021/la303101x | *Langmuir* 2013, 29, 561−569

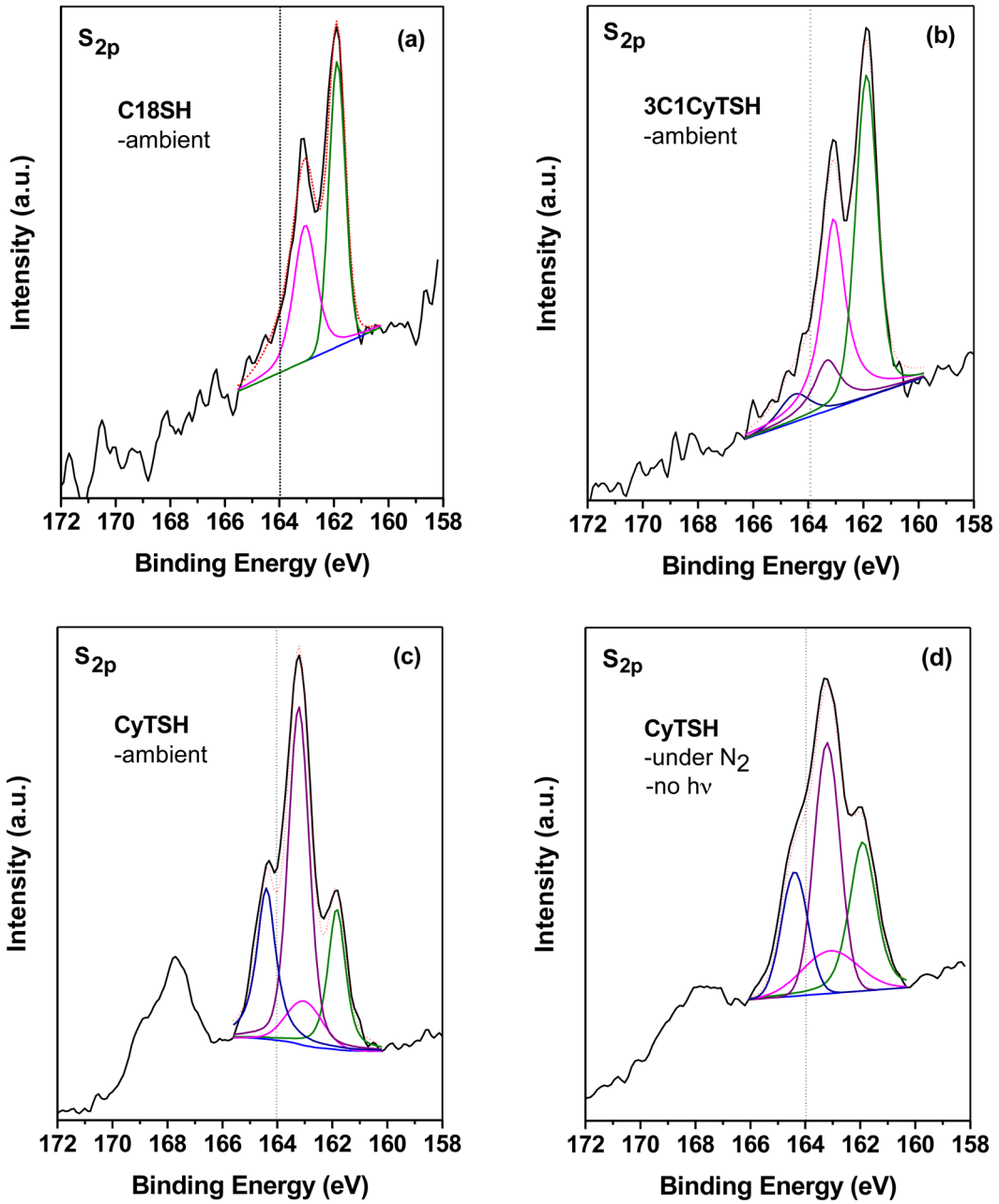

Figure 3. XPS spectra of films generated from (a) octadecanethiol (**C18SH**) in ethanol, and (b) **3C1CyTSH** and (c, d) **CyTSH** in THF. Ambient laboratory conditions were 25 °C, light, and air. Green and pink lines represent $S_{2p^3/_2}$ and $S_{2p^1/_2}$ for bound thiolate, respectively. Purple and navy lines represent $S_{2p^3/_2}$ and $S_{2p^1/_2}$ for unbound thiol and/or disulfide species, respectively.[45,47].

Scheme 2. Axial and Equatorial Conformations of 3C1CyTSH and CyTSH

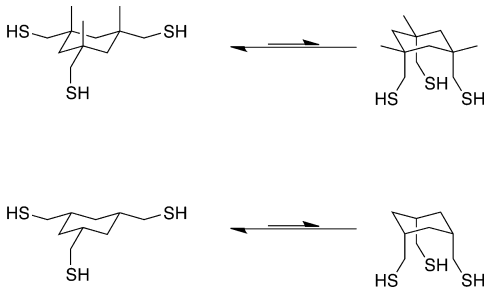

orientation(s) of the adsorbed molecules.[30,54] For SAMs derived from normal alkanethiols, the $\nu_a^{CH_2}$ and $\nu_s^{CH_3}$ transition dipoles are oriented nearly parallel to the surface normal (true for $\nu_s^{CH_3}$ especially for even-numbered SAMs)[55] leading to strong absorptions for these modes.[30] For 3C3CyTSH, however, the intensity of the $\nu_a^{CH_2}$ band weakens upon adsorption while the intensity of the $\nu_a^{CH_3}$ remains relatively strong (see Figure 4). These results provide strong support that 3C3CyTSH binds to the gold surface with the methylene thiol moieties pointed downward and the methyl groups pointed upward, but titled from the surface normal (i.e., equatorial rather than axial conformations for the methyl groups; see Scheme 2).

dx.doi.org/10.1021/la303101x | *Langmuir* 2013, 29, 561−569

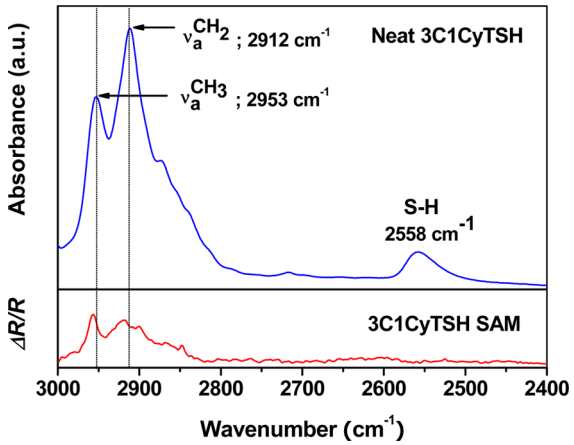

Figure 4. Comparison of the C−H stretching region between the transmission FT-IR spectrum of **3C1CyTSH** as neat oil and the PM-IRRAS spectrum of the **3C1CyTSH** SAM derived from **3C1CyTSH** in THF.

Additionally, Figure 5 compares the PM-IRRAS spectrum of thin films derived from **3C1CyTSH** to those of films derived

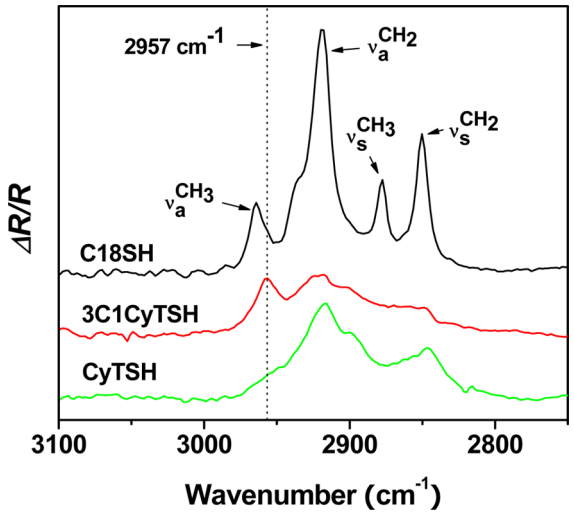

Figure 5. C−H stretching region of the PM-IRRAS spectra of SAMs derived from **C18SH**, **3C1CyTSH**, and **CyTSH**.

from *n*-octadecanethiol (**C18SH**) and **CyTSH**. Notably, the band at ~2957 cm^{-1} is absent in the spectrum for **CyTSH**, which supports our assignment of this band as $\nu_a^{CH_3}$ for **3C1CyTSH**.

Measurements of Film Thickness. Ellipsometry is one of the principle tools used to determine the average monolayer thickness and follow the progress of the film growth.[34] In the present study, we assumed a refractive index of 1.45 for all films examined. However, since the surface coverage and chemical composition can substantially influence the refractive index values,[34] we also used XPS to determine the thickness of films. In these measurements, the amount of adsorbate on the surface of the gold substrate can attenuate the XPS signal for Au. Thus, the thickness of monolayer films can be calculated using the relative intensities of Au_{4f} and C_{1s} peaks from the XPS spectra. In this procedure, we measured the intensities of the Au_{4f} peak of the underlying gold substrate for each sample and set the binding energy of the Au_{4f} peak to 84.0 eV as a reference. Also, we used the monolayer derived from **C18SH** (with a known thickness of 22 Å)[48] as a standard for comparison. The film thicknesses were calculated using eq 1:

$$\frac{\frac{I_C^S}{I_{Au}^S}}{\frac{I_C^R}{I_{Au}^R}} = \frac{1 - e^{-d_S/\lambda_C(E_{kin,C})}}{e^{-d_S/\lambda_C(E_{kin,Au})}} \cdot \frac{e^{-d_R/\lambda_C(E_{kin,Au})}}{1 - e^{-d_R/\lambda_C(E_{kin,C})}} \quad (1)$$

where d_R is the thickness of the **C18SH** SAM, d_S is the thickness of the SAM under investigation, and the I term represents the intensities for C_{1s} "C" and Au_{4f} "Au" for sample "S" and reference "R". The λ terms are the escape depths of the electrons for the different kinetic energies, calculated using the NIST database.[56]

Table 2 provides a comparison of the film thickness determined by ellipsometry and by XPS. The results show

Table 2. Thickness of SAMs Determined by Ellipsometry and by XPS

		thickness (Å)	
adsorbate	solvent	ellipsometric[a]	XPS
C18SH	EtOH	21	22[48]
CyTSH	THF	13	15
3C1CyTSH	THF	4	5
3C1CyTSH	EtOH	4	4
3C1CyTSH	*i*-Pr ether	6	6
3C1CyTSH	DME	3	5
3C1CyTSH	toluene	4	4

[a]Measured values were reproducible within ±2 Å of the reported values.

that the methods are largely consistent. Notably, **3C1CyTSH** generates a monolayer film that is thinner than the SAM generated by **C18SH**. This result was expected given that **3C1CyTSH** possesses roughly a 3-carbon chain length while **C18SH** possesses an 18-carbon chain length. Importantly, the thickness of the **3C1CyTSH** SAM (5 ± 1 Å) is consistent with its molecular dimensions calculated by molecular modeling assuming a planar conformation.[57] In contrast, the **CyTSH** adsorbate, which gives films with thicknesses ranging from 11 to 15 Å, appears to form multilayer films via the formation of intermolecular disulfides as indicated by the XPS data in Figure 3c,d.

Interfacial Wettability. The wettability of the films was explored using water, hexadecane, decalin, and diisopropyl ether as contacting liquids. The results of contact angle measurement are displayed in Table 3. The contact angles of

Table 3. Advancing Contact Angles (θ_a) of Water (H_2O), Hexadecane (HD), Decalin (DL), and Diisopropyl ether (DIPE) on SAMs Derived from the Adsorption of C18SH in EtOH and CyTSH and 3C1CyTSH in THF

	contact angle (θ_a)			
adsorbate	H_2O	HD	DL	DIPE
C18SH	114	50	54	---[a]
CyTSH	74	---	---	---
3C1CyTSH	78	---	---	---
bare gold	74	---	---	---

[a]The symbol --- indicates that the film was wet by the contacting liquid (θ_a < 10°).

dx.doi.org/10.1021/la303101x | *Langmuir* 2013, 29, 561−569

the films generated from **CyTSH** are low (comparable to "bare" gold) due to the presence of oxidized sulfur species as indicated by the XPS analyses described above. In contrast, the low contact angle values for the films generated from **3C1CyTSH** can be attributed to the fact that these films are extremely thin. Consequently, the probe liquids interact strongly with the underlying gold surface, which enhances the wettability of the films.[59] This interpretation is consistent with XPS and ellipsometric thickness values.

CONCLUSIONS

Two tridentate alkanethiols with cyclohexyl headgroups were synthesized and used to prepare thin films on gold, which were characterized by ellipsometry, contact angle goniometry, PM-IRRAS, and XPS. While the adsorption of **CyTSH** led to multilayer films containing oxidized sulfur species, the adsorption of **3C1CyTSH** led to monolayer films with ∼90% of the sulfur atoms bound to gold. The striking difference can be attributed to the presence of the methyl groups in **3C1CyTSH**, which restrict the conformational flexibility of the cyclohexane ring and thereby significantly enhance its chemisorption to gold. When taken as a whole, the results suggest that the tridentate **3C1CyTSH** architecture can be used to generate strongly bound SAMs on gold.

AUTHOR INFORMATION

Corresponding Author

*E-mail: trlee@uh.edu.

Notes

The authors declare no competing financial interest.

ACKNOWLEDGMENTS

We thank the National Science Foundation (DMR-0906727), the Robert A. Welch Foundation (grant no. E-1320), and the Texas Center for Superconductivity at the University of Houston for generous support. We also thank the Royal Thai Government for supporting the predoctoral studies of Mr. Burapol Singhana, and we thank Dr. Andrew C. Jamison and Mr. Johnson Hoang for their generous assistance.

REFERENCES

(1) Love, J. C.; Estroff, L. A.; Kriebel, J. K.; Nuzzo, R. G.; Whitesides, G. M. Self- Assembled Monolayers of Thiolates on Metals as a Form of Nanotechnology. *Chem. Rev.* **2005**, *105*, 1103−1169.

(2) Ulman, A. *An Introduction to Ultrathin Organic Films*; Academic: Boston, MA, 1991.

(3) Ulman, A. Formation and Structure of Self-Assembled Monolayers. *Chem. Rev.* **1996**, *96*, 1533−1554.

(4) Schreiber, F. Structure and Growth of Self-Assembling Monolayers. *Prog. Surf. Sci.* **2000**, *65*, 151−256.

(5) Garg, N.; Lee, T. R. Self-Assembled Monolayers Based on Chelating Aromatic Dithiols on Gold. *Langmuir* **1998**, *14*, 3815−3819.

(6) Scherer, J.; Vogt, M. R.; Magnussen, O. M.; Behm, R. J. Corrosion of Alkanethiol-Covered Cu(100) Surfaces in Hydrochloric Acid Solution Studied by in-Situ Scanning Tunneling Microscopy. *Langmuir* **1997**, *13*, 7045−7051.

(7) Cox, J. D.; Curry, M. S.; Skirboll, S. K.; Gourley, P. L.; Sasaki, D. Y. Surface Passivation of a Microfluidic Device to Glial Cell Adhesion: A Comparison of Hydrophobic and Hydrophilic SAM Coatings. *Biomaterials* **2002**, *23*, 929−935.

(8) Wilson, R. The Use of Gold Nanoparticles in Diagnostics and Detection. *Chem. Soc. Rev.* **2008**, *37*, 2028−2045.

(9) Riehemann, K.; Schneider, S. W.; Luger, T. A.; Godin, B.; Ferrari, M.; Fuchs, H. Nanomedicine−Challenge and Perspectives. *Angew. Chem., Int. Ed.* **2009**, *48*, 872−897.

(10) Dykman, L.; Khlebtsov, N. Gold Nanoparticles in Biomedical Applications: Recent Advances and Perspectives. *Chem. Soc. Rev.* **2011**, *41*, 2256−2282.

(11) Dreaden, E. C.; Alkilany, A. M.; Huang, X.; Murphy, C. J.; El-Sayed, M. A. The Golden Age: Gold Nanoparticles for Biomedicine. *Chem. Soc. Rev.* **2011**, *41*, 2740−2779.

(12) Kim, S.; Choi, G. Y.; Ulman, A.; Fleischer, C. Effect of Chemical Functionality on Adhesion Hysteresis. *Langmuir* **1997**, *13*, 6850−6856.

(13) Houston, J. E.; Doelling, C. M.; Vanderlick, T. K.; Hu, Y.; Scoles, G.; Wenzl, I.; Lee, T. R. Comparative Study of the Adhesion, Friction, and Mechanical Properties of CF_3- and CH_3-Terminated Alkanethiol Monolayers. *Langmuir* **2005**, *21*, 3926−3932.

(14) Xiao, X.; Hu, J.; Charych, D. H.; Salmeron, M. Chain Length Dependence of the Frictional Properties of Alkylsilane Molecules Self-Assembled on Mica Studied by Atomic Force Microscopy. *Langmuir* **1996**, *12*, 235−237.

(15) Xia, Y.; Whitesides, G. M. Soft Lithography. *Angew. Chem., Int. Ed.* **1998**, *37*, 550−575.

(16) Gates, B. D.; Xu, Q.; Stewart, M.; Ryan, D.; Willson, C. G.; Whitesides, G. M. New Approaches to Nanofabrication: Molding, Printing, and Other Techniques. *Chem. Rev.* **2005**, *105*, 1171−1196.

(17) *Encyclopedia of Electrochemistry*; Fujihira, M., Rubinstein, I., Rusling, J. F., Eds.; Wiley-VCH: Weinheim, Germany, 2007; Vol. *10*, Chapter 1.

(18) DiBenedetto, S. A.; Facchetti, A.; Ratner, M. A.; Marks, T. J. Molecular Self-Assembled Monolayers and Multilayers for Organic and Unconventional Inorganic Thin-Film Transistor Applications. *Adv. Mater.* **2009**, *21*, 1407−1433.

(19) Miozzo, L.; Yassar, A.; Horowitz, G. Surface Engineering for High Performance Organic Electronic Devices: The Chemical Approach. *J. Mater. Chem.* **2010**, *20*, 2513−2538.

(20) Halik, M.; Hirsch, A. The Potential of Molecular Self-Assembled Monolayers in Organic Electronic Devices. *Adv. Mater.* **2011**, *23*, 2689−2695.

(21) Srisombat, L.; Jamison, A. C.; Lee, T. R. Stability: A Key Issue for Self-Assembled Monolayers on Gold as Thin-Film Coatings and Nanoparticle Protectants. *Colloids Surf., A* **2011**, *390*, 1−19.

(22) Giljohann, D. A.; Seferos, D. S.; Daniel, W. L.; Massich, M. D.; Patel, P. C.; Mirkin, C. A. Gold Nanoparticles for Biology and Medicine. *Angew. Chem., Int. Ed.* **2010**, *49*, 3280−3294.

(23) Pissuwan, D.; Niidome, T.; Cortie, M. B. The Forthcoming Applications of Gold Nanoparticles in Drug and Gene Delivery Systems. *J. Controlled Release* **2011**, *149*, 65−71.

(24) Chinwangso, P.; Jamison, A. C.; Lee, T. R. Multidentate Adsorbates for Self-Assembled Monolayer Films. *Acc. Chem. Res.* **2011**, *44*, 511−519.

(25) Schoenfisch, M. H.; Pemberton, J. E. Air Stability of Alkanethiol Self-Assembled Monolayers on Silver and Gold Surfaces. *J. Am. Chem. Soc.* **1998**, *120*, 4502−4513.

(26) Shon, Y.-S.; Lee, T. R. A Steady State Kinetic Model Can Be Used to Describe the Growth of Self-Assembled Monolayers (SAMs) on Gold. *J. Phys. Chem. B* **2000**, *104*, 8182−8191.

(27) Shon, Y.-S.; Colorado, R., Jr.; Williams, C. T.; Bain, C. D.; Lee, T. R. Low Density Self-Assembled Monolayers on Gold Derived from Chelating 2-Monoalkylpropane-1,3-dithiols. *Langmuir* **2000**, *16*, 541−548.

(28) Garg, N.; Carrasquilo-Molina, E.; Lee, T. R. Self-Assembled Monolayers Composed of Aromatic Thiols on Gold: Structural Characterization and Thermal Stability in Solution. *Langmuir* **2002**, *18*, 2717−2726.

(29) Park, J.-S.; Smith, A. C.; Lee, T. R. Loosely Packed Self-Assembled Monolayers on Gold Generated from 2-Alkyl-2-methyl-propane-1,3-dithiols. *Langmuir* **2004**, *20*, 5829−5836.

(30) Park, J.-S.; Vo, A. N.; Barriet, D.; Shon, Y.-S.; Lee, T. R. Systematic Control of the Packing Density of Self-Assembled

Monolayers Using Bidentate and Tridentate Chelating Alkanethiols. *Langmuir* **2005**, *21*, 2902−2911.
(31) Zhang, S.; Leem, G.; Srisombat, L.; Lee, T. R. Rationally Designed Ligands that Inhibit the Aggregation of Large Gold Nanoparticles in Solution. *J. Am. Chem. Soc.* **2008**, *130*, 113−120.
(32) Chinwangso, P. Self-Assembled Monolayers Generated from Custom-Tailored Spiroalkanedithiols Offer Unprecedented Multi-Component Interfaces. Ph.D. Thesis, University of Houston, Houston, TX, 2009.
(33) Nuzzo, R. G.; Allara, D. L. Adsorption of Bifunctional Organic Disulfides on Gold Surfaces. *J. Am. Chem. Soc.* **1983**, *105*, 4481−4483.
(34) Nuzzo, R. G.; Fusco, F. A.; Allara, D. L. Spontaneously Organized Molecular Assemblies. 3. Preparation and Properties of Solution Adsorbed Monolayers of Organic Disulfides on Gold Surfaces. *J. Am. Chem. Soc.* **1987**, *109*, 2358−2368.
(35) Whitesell, J. K.; Chang, H. K. Directionally Aligned Helical Peptides on Surfaces. *Science* **1993**, *261*, 73−76.
(36) Stewart, M. H.; Susumu, K.; Mei, B. C.; Medintz, I. L.; Delehanty, J. B.; Blanco-Canosa, J. B.; Dawson, P. E.; Mattoussi, H. Multidentate Poly(ethylene glycol) Ligands Provide Colloidal Stability to Semiconductor and Metallic Nanocrystals in Extreme Conditions. *J. Am. Chem. Soc.* **2010**, *132*, 9804−9813.
(37) Srisombat, L.; Park, J.-S.; Zhang, S.; Lee, T. R. Preparation, Characterization, and Chemical Stability of Gold Nanoparticles Coated with Mono-, Bis-, and Tris-Chelating Alkanethiols. *Langmuir* **2008**, *24*, 7750−7754.
(38) Kittredge, K. W.; Minton, M. A.; Fox, M. A.; Whitesell, J. K. α-Helical Polypeptide Films Grown from Sulfide or Thiol Linkers on Gold Surfaces. *Helv. Chim. Acta* **2002**, *85*, 788−798.
(39) Kitagawa, T.; Idomoto, Y.; Matsubara, H.; Hobara, D.; Kakiuchi, T.; Okazaki, T.; Komatsu, K. Rigid Molecular Tripod with an Adamantane Framework and Thiol Legs. Synthesis and Observation of an Ordered Monolayer on Au(111). *J. Org. Chem.* **2006**, *71*, 1362−1369.
(40) Katano, S.; Kim, Y.; Matsubara, H.; Kitagawa, T.; Kawai, M. Hierarchical Chiral Framework Based on a Rigid Adamantane Tripod on Au(111). *J. Am. Chem. Soc.* **2007**, *129*, 2511−2515.
(41) Ye, Q.; Komarov, I. V; Kirby, A. J.; Jones, M., Jr. 3,5,7-Trimethyl-1-azatricyclo[3.3.1.1(3,7)]decan-2-ylidene, an Aminocarbene without π Conjugation. *J. Org. Chem.* **2002**, *67*, 9288−9294.
(42) Tajc, S. G.; Miller, B. L. A Designed Receptor for pH-Switchable Ion Binding in Water. *J. Am. Chem. Soc.* **2006**, *128*, 2532−2533.
(43) Jeong, K. S.; Tjivikua, T.; Muehldorf, A.; Deslongchamps, G.; Famulok, M.; Rebek, J., Jr. Convergent Functional Groups. 10. Molecular Recognition of Neutral Substrates. *J. Am. Chem. Soc.* **1991**, *113*, 201−209.
(44) Shon, Y.-S.; Lee, S.; Colorado, R., Jr.; Perry, S. S.; Lee, T. R. Spiroalkanedithiol-Based SAMs Reveal Unique Insight into the Wettabilities and Frictional Properties of Organic Thin Films. *J. Am. Chem. Soc.* **2000**, *122*, 7556−7563.
(45) Duwez, A.-S. Exploiting Electron Spectroscopies to Probe the Structure and Organization of Self-Assembled Monolayer: a Review. *J. Electron Spectrosc. Relat. Phenom.* **2004**, *134*, 97−138.
(46) Laibinis, P. E.; Whitesides, G. M.; Allara, D. L.; Tao, Y. T.; Parikh, A. N.; Nuzzo, R. G. Comparison of the Structures and Wetting Properties of Self-Assembled Monolayers of *n*- Alkanethiols on the Coinage Metal Surfaces, Cu, Ag, Au[1]. *J. Am. Chem. Soc.* **1991**, *113*, 7152−7167.
(47) Castner, D. G.; Hinds, K.; Grainger, D. W. X-ray Photoelectron Spectroscopy Sulfur 2p Study of Organic Thiol and Disulfide Binding Interactions with Gold Surfaces. *Langmuir* **1996**, *12*, 5083−5086.
(48) Bain, C. D.; Troughton, E. B.; Tao, Y. T.; Evall, J.; Whitesides, G. M.; Nuzzo, R. G. Formation of Monolayer Films by the Spontaneous Assembly of Organic Thiols from Solution onto Gold. *J. Am. Chem. Soc.* **1989**, *111*, 321−335.
(49) Carey, F. A.; Sundberg, R. J. *Advanced Organic Chemistry*, 3rd ed.; Plenum: New York, 1990.
(50) Willey, T. M.; Vance, A. L.; van Buuren, T.; Bostedt, C.; Terminello, L. J.; Fadley, C. S. Rapid Degradation of Alkanethiol-Based Self-Assembled Monolayers on Gold in Ambient Laboratory Conditions. *Surf. Sci.* **2005**, *576*, 188−196.
(51) Hofmann, A.; Ren, R.; Lough, A.; Fekl, U. Highly Substituted Cyclohexanes: Strong Proximity Effects Influence Synthetic Access to 1,3,5-Tris(bromomethyl)-1,3,5-trialkylcyclohexanes (Alkyl = Methyl, *n*-Propyl). *Tetrahedron Lett.* **2006**, *47*, 2607−2610.
(52) Anslyn, E. V.; Dougherty, D. A. *Modern Physical Organic Chemistry*; University Science Books: Sausalito, CA, 2004.
(53) Bain, C. D.; Whitesides, G. M. Formation of Monolayers by the Coadsorption of Thiols on Gold: Variation in the Length of the Alkyl Chain. *J. Am. Chem. Soc.* **1989**, *111*, 7164−7175.
(54) Snyder, R. G.; Strauss, H. L.; Elliger, C. A. Carbon-Hydrogen Stretching Modes and the Structure of n-Alkyl Chains. 1. Long, Disordered Chains. *J. Phys. Chem.* **1982**, *86*, 5145.
(55) Tao, F.; Bernasek, S. L. Understanding Odd-Even Effects in Organic Self-Assembled Monolayers. *Chem. Rev.* **2007**, *107*, 1408−1453 (and references therein).
(56) Hallman, L.; Bashir, A.; Strunskus, T.; Adelung, R.; Woll, Ch.; Tuczek, F. Self-Assembled Monolayers of Benzylmercaptan and *p*-Cyanobenzylmercaptan on Au(111) Surfaces: Structural and Spectroscopic Characterization. *Langmuir* **2008**, *24*, 5726−5733.
(57) For calculating the theoretical film thicknesses based on the implementation of algorithm of simple geometry and trigonometry, we assumed that this adsorbate has a planar conformation on flat gold. The following data were used: $C_{methyl}-C_{cyclohexane}$ ∼1.5 Å, $C_{methylene}-S$ ∼1.8 Å,[58] S−Au ∼2.5 Å,[58] <CCC ∼109.5. Based on these values, the estimated thickness for **3C1CyTSH** was calculated to be 1.5 + 1.5 sin(109.5−90) + 1.8 + 2.5 = 6.3 Å.
(58) Cao, Y.; Ge, Q.; Dyer, D. J.; Wang, L. Steric Effects on the Adsorption of Alkylthiolate Self-Assembled Monolayers on Au(111). *J. Phys Chem. B* **2003**, *107*, 3803−3807.
(59) Miller, W. J.; Abbott, N. L. Influence of van der Waals Forces from Metallic Substrates on Fluids Supported on Self-Assembled Monolayers Formed from Alkanethiols. *Langmuir* **1997**, *13*, 7106−7114.